Supplementary Information (SI) DOI: https:/

Designing of MOFs-Based Green Nanomaterials for Enhanced Pathogen Resistance and Pesticide Degradation in Tomato Plants

Shoaib Khan[1], Aoxue Wang[1]✉, Jiayin Liu[1]✉, Iltaf Khan[2]✉, Samreen Sadiq[3], Aftab Khan[4], Waleed Yaseen[5], Saeed Zaman[6], Abdul Mueed[7], Yuanyang Miao[1]

[1]College of Horticulture and Landscape Architecture, Northeast Agricultural University, Harbin, 150030, China
[2]School of Environmental & Chemical Engineering, Jiangsu University of Science and Technology, Zhenjiang, 212100, China
[3]Jiangsu Key Laboratory of Sericultural and Animal Biotechnology, School of Biotechnology, Jiangsu University of Science and Technology, Zhenjiang, 212100, China
[4]Beijing Advanced Innovation Center for Soft Matter Science and Engineering, State Key Laboratory of Chemical Resource Engineering, School of Materials Science and Engineering, Beijing University of Chemical Technology, Beijing, 100029, China
[5]School of Chemistry and Chemical Engineering, Department of Pharmacy, Jiangsu University, Zhenjiang 212013, PR China
[6]College of Chemistry, Liaoning University, Shenyang, 110036, China
[7]State Key Laboratory of Food Science and Technology, Nanchang University, Nanchang, 330047, China

✉Corresponding Email (s): axwang@neau.edu.cn, liujiayin@neau.edu.cn , doctoriltafkhan@just.edu.cn

Table of Contents

1. Experimental Part

1.1 Photoluminescence spectroscopy measurement

By using a Spectro fluorophotometer, the photoluminescence (PL) spectra of the synthesized samples were investigated. The excitation and emission wavelengths were adjusted to 248 nm and 600 nm, respectively. The excitation and emission

scanning parameters remained constant at a specific value that aligned with the absorption peak of the material.

1.2 Free radicals trapping experiments

Extensive studies were carried out to validate the photocatalytic mechanism and degradation pathways of GLY and ACPH. Three scavenger species were employed to detect reactive species: EDTA-2Na, IPA, and benzoquinone to identify photogenerated holes, hydroxyl radicals, and superoxide radicals respectively. In the typical experiment, a small quantity of scavenger solutions was added to 50 mL solutions of GLY and ACPH having a concentration of 10 mg/L^{-1}. This mixture was then exposed to irradiation for a duration of 1 h. Afterward, a 5 mL sample was taken, filtered, and investigated for pesticide concentration using a 400 W Xenon lamp at 497 nm.

1.3 Fourier-transform infrared spectroscopy

The composition and molecular structure of samples were measured using the FT-IR spectrometer, with potassium bromide used as the diluent. The samples required exposure to specific frequencies of infrared radiation, which led to the stimulation of molecular vibrations or rotations. The analysis of the position of spectral absorption peaks enabled the classification of functional groups.

1.4 BET surface area and pore diameter measurement

The surface area of the samples was measured using a Micromeritics Tristar II 3020 analyzer by analyzing nitrogen adsorption-desorption at a temperature of -196 °C. in the typical experiment, the sample weighing 0.1 g received pretreatment at a temperature of 150 °C to remove any moisture. Afterward, the samples that were previously pretreated (ZIF-67, SnO_2, and SnO_2/ZIF-67) were carefully placed in an apparatus designed to measure the BET surface area.

2. Supporting Figures

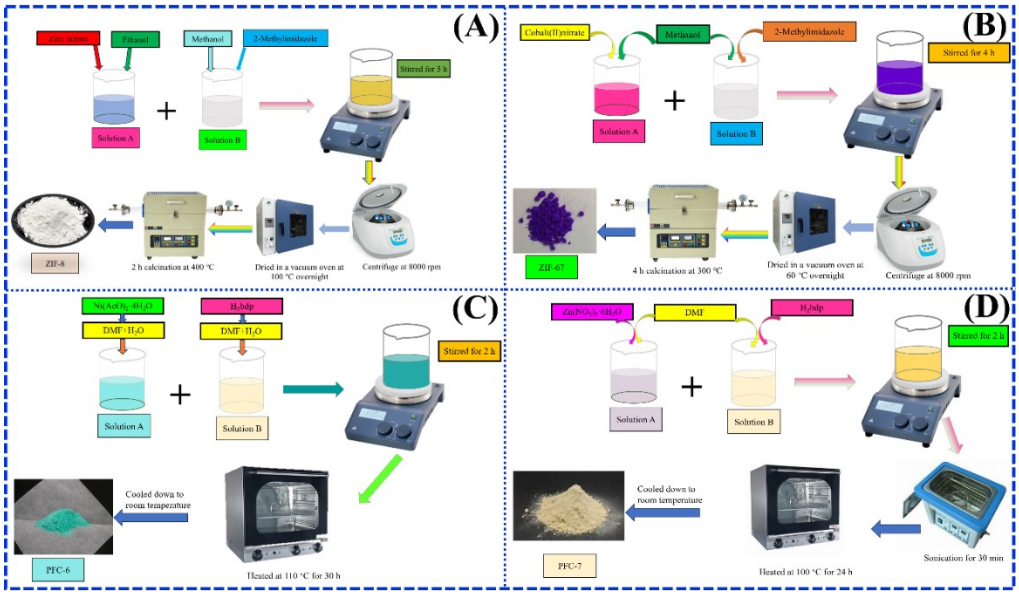

Figure. S1. Schematic representation for synthesis of MOFs (ZIF-8, ZIF-67, PFC-6, PFC-7).

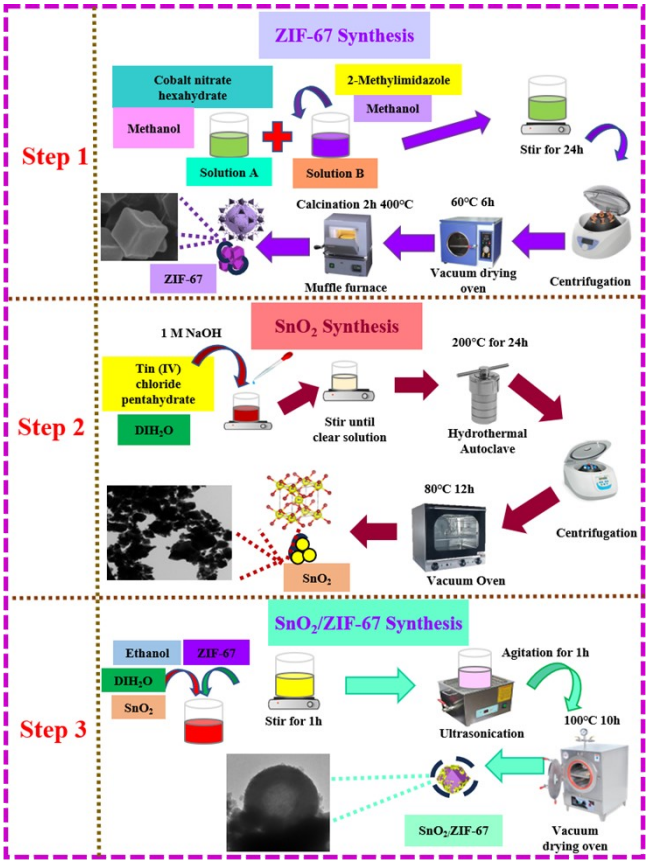

Figure. S2. Schematic representation for synthesis ZIF-67, SnO_2, and SnO_2/ZIF-67 nanocomposite.

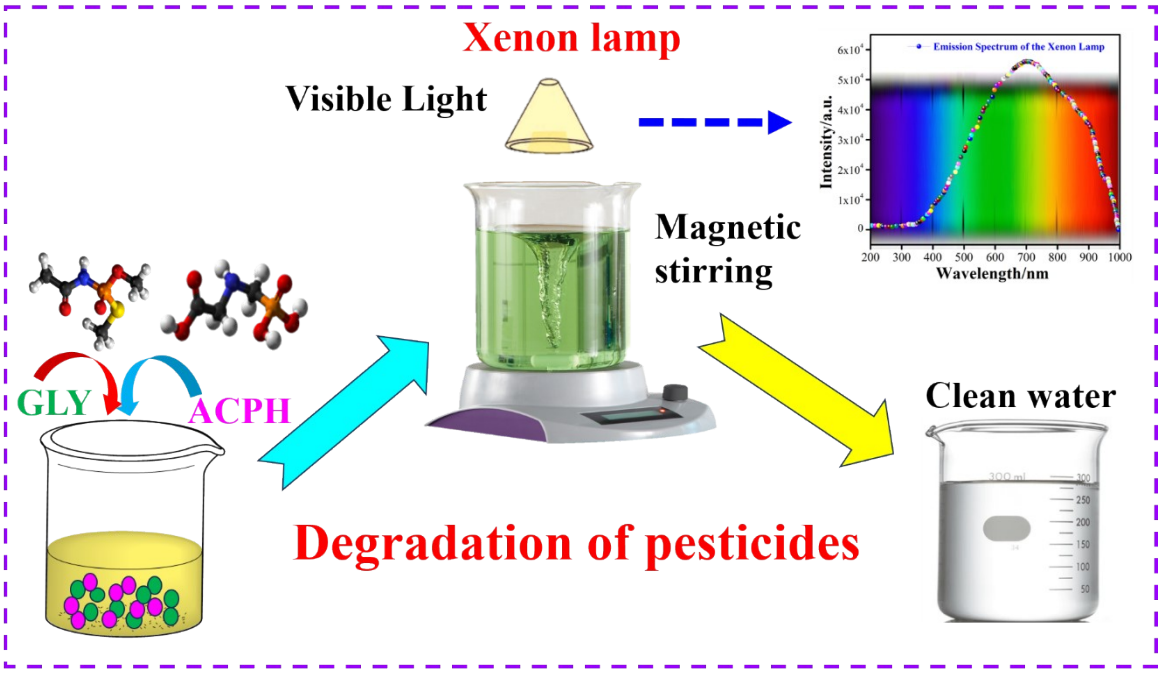

Figure. S3. Diagrammatical depiction of degradation of pesticides.

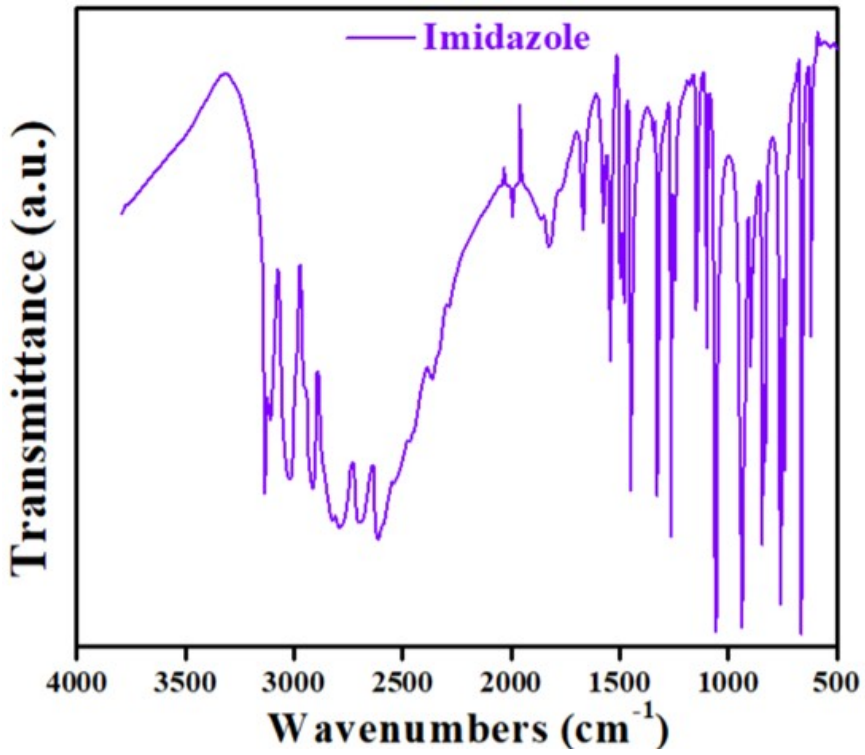

Figure. S4. IR spectrum of the imidazole.

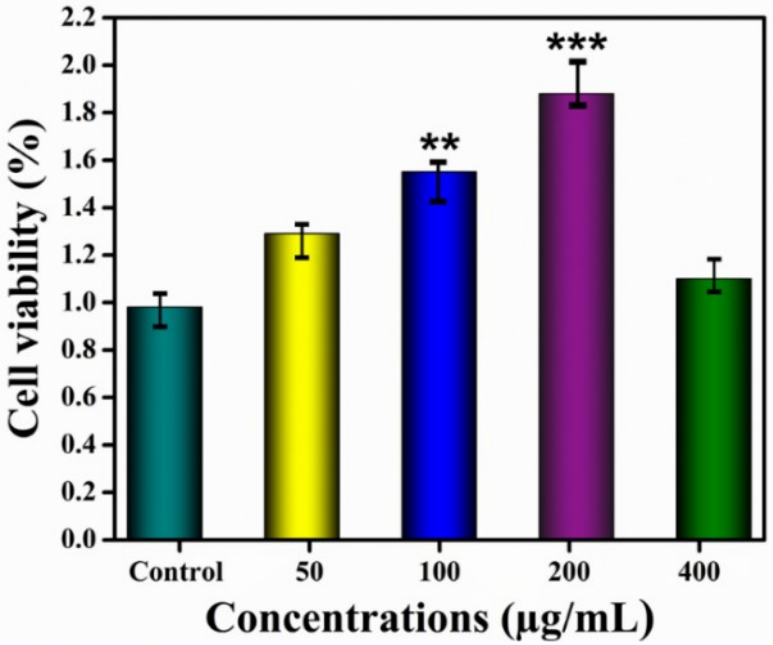

Figure. S5. The bar graph assessing the percentage of cell viability across four different concentrations using the CCK-8 assay. The concentration range of nanosheets (BPNSs) is between 50 and 400 μg/mL, with incubation periods of 4 h. The control consisted of the cell line that had no additives at all (0 μg/mL). The data are shown with standard deviation (n = 4; mean ± SD, ANOVA/Tukey's test; *P < 0.05, **P < 0.01, ***P < 0.001).

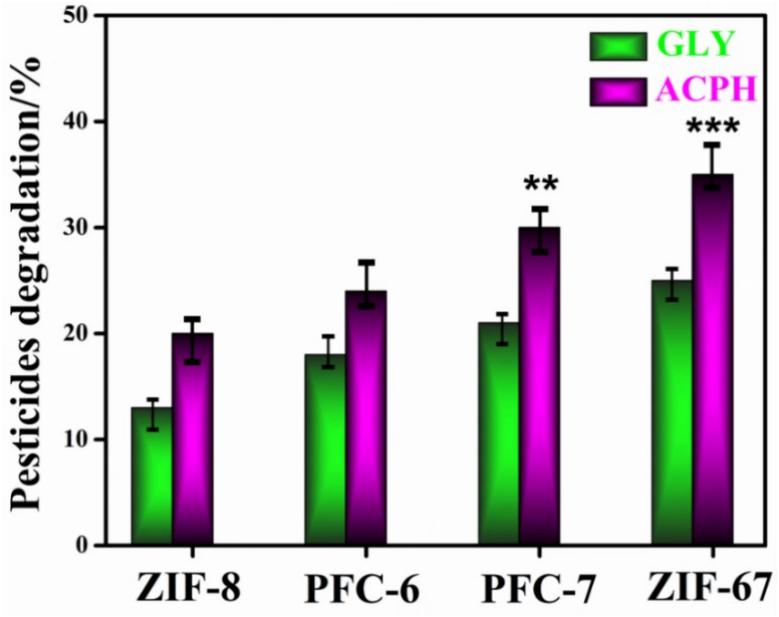

Figure. S6. Pesticide (GLY and ACPH) degradation over MOFs (ZIF-8, PFC-6, PFC-7, ZIF-67). The values are presented as the mean ± SD, with a sample size of n=4. Values are found to be statistically significant at a significance level of P <0.05. Error bars represent the mean SEM; ** P < 0.01, *** P < 0.001.

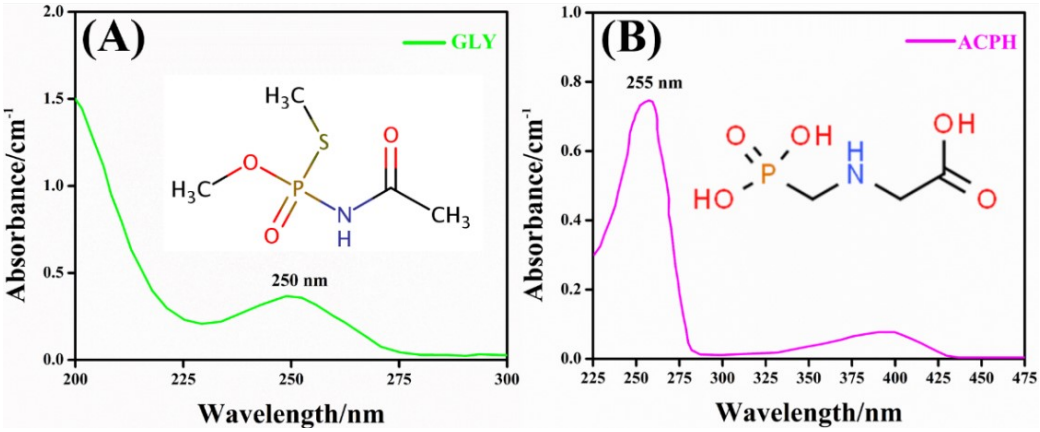

Figure. S7. UV absorbance model spectra of GLY (A) and ACPH (B).

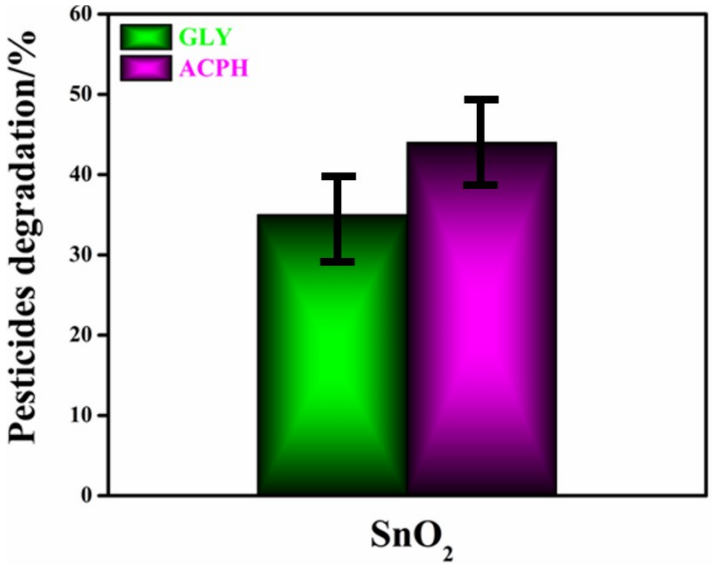

Figure. S8. GLY and ACPH degradation activities over SnO_2.

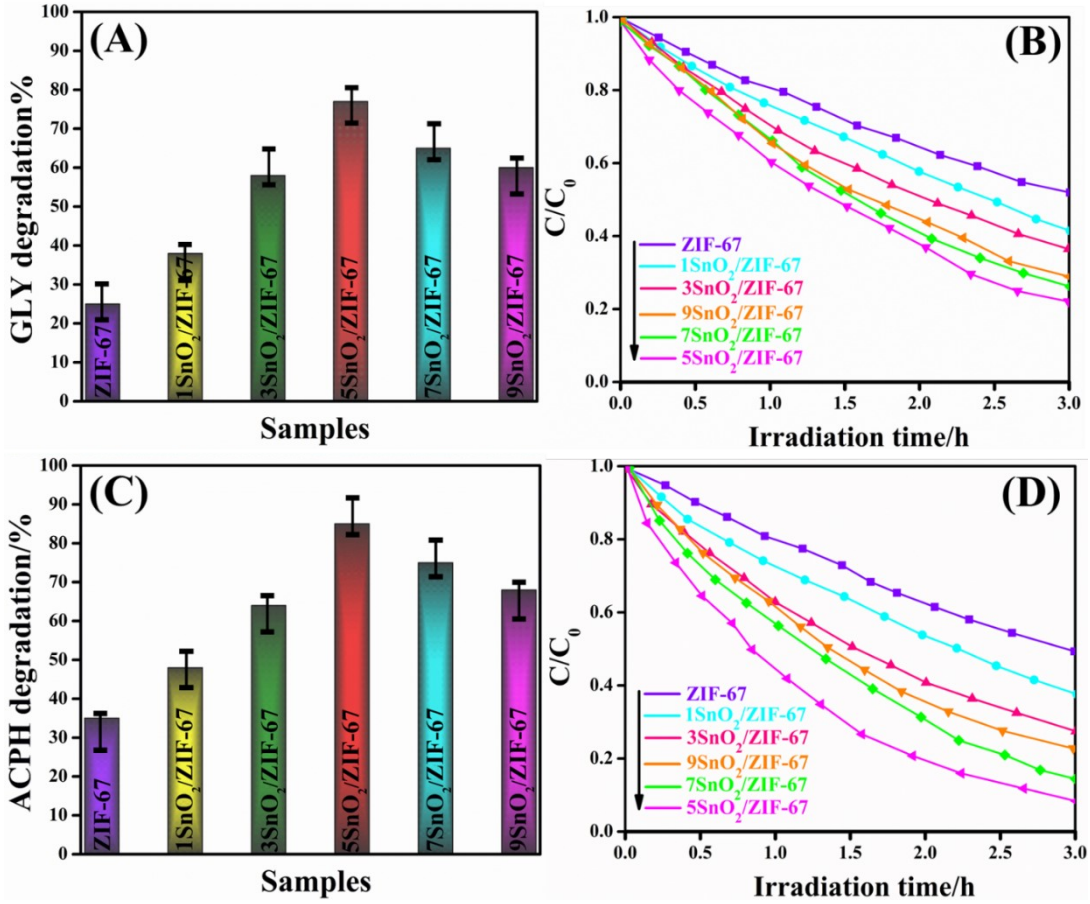

Figure. S9. GLY degradation activities (A), GLY time-dependent activities (B), ACPH degradation activities (C), and ACPH time-dependent activities (D) over ZIF-67 and γSnO_2/ZIF-67.

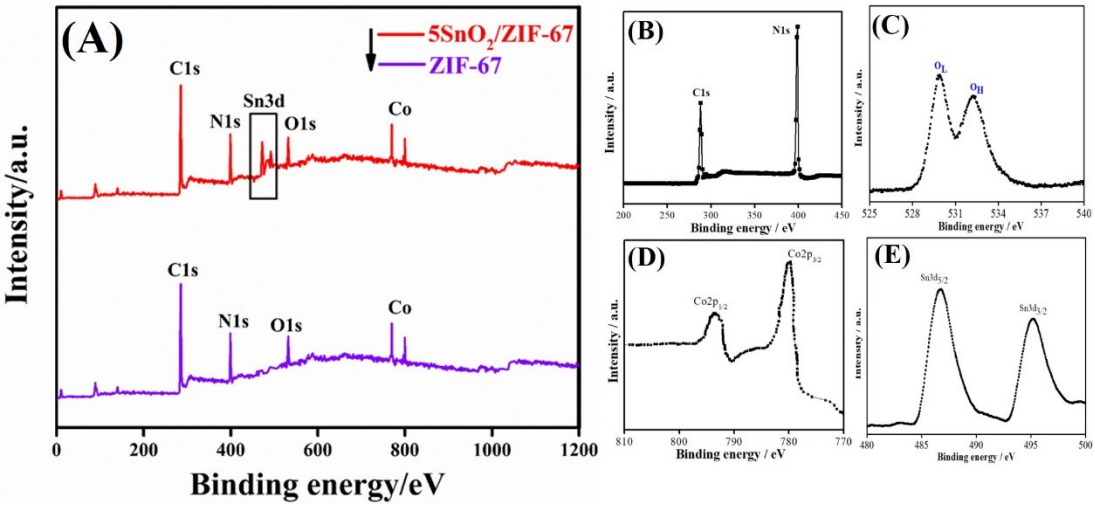

Figure. S10. XPS survey spectra of ZIF-67 and 5SnO_2/ZIF-67 (A), High-resolution spectra of C-N(B), O (C), Co(D) and Sn(E).

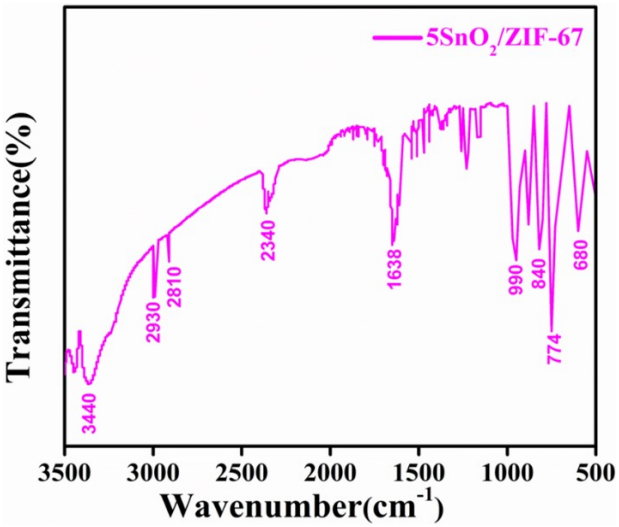

Figure. S11. FT-IR Spectra of 5ZIF-67/SnO_2.

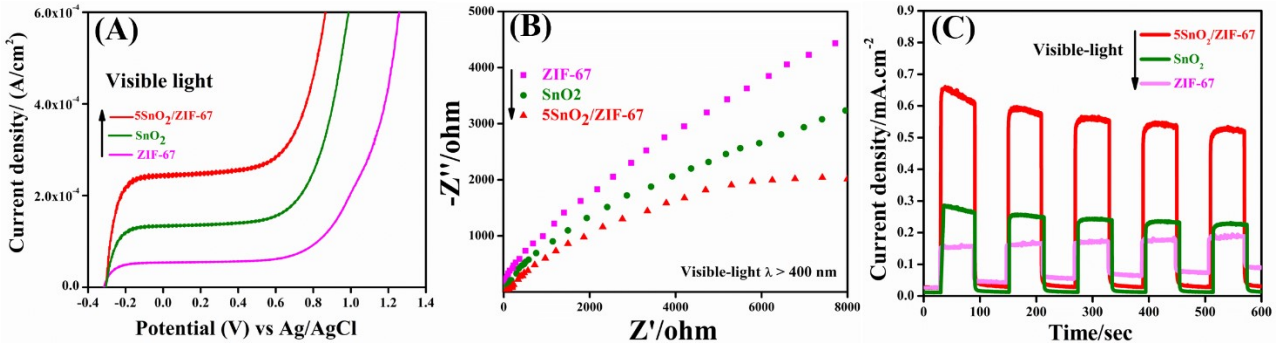

Figure. S12. PEC I-V curves (A), Electrochemical Impedance Spectra (EIS) (B), PEC I-t curves (C) of Pristine ZIF-67, SnO_2 and 5SnO/ZIF-67 nanocomposite.

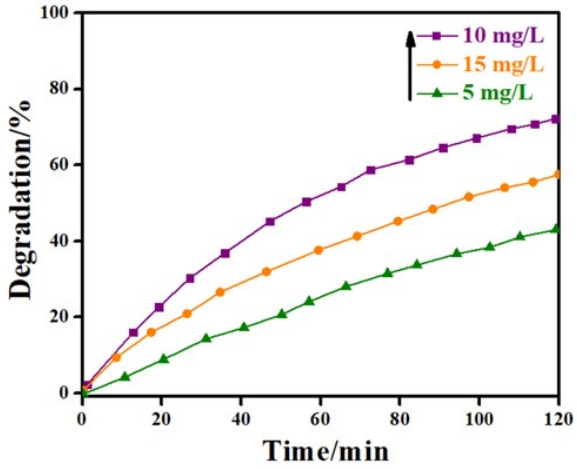

Figure. S13. GLY degradation activity tests with different concentrations over 5SnO/ZIF-67 nanocomposite.

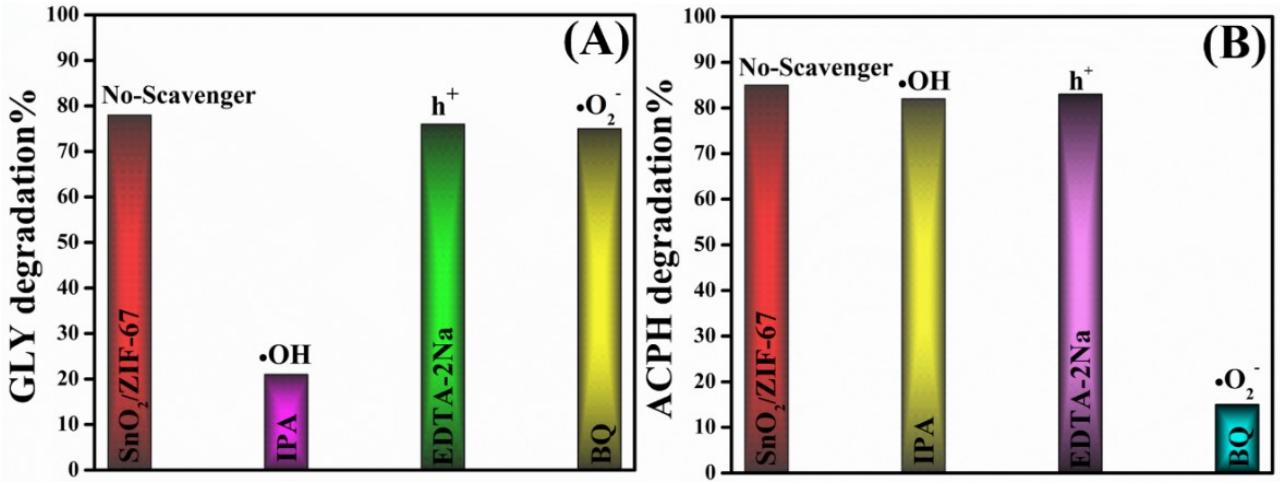

Figure. S14. Scavenger test for GLY (A), and ACPH (B) degradation over $5SnO_2$ /ZIF-67 nanocomposite.

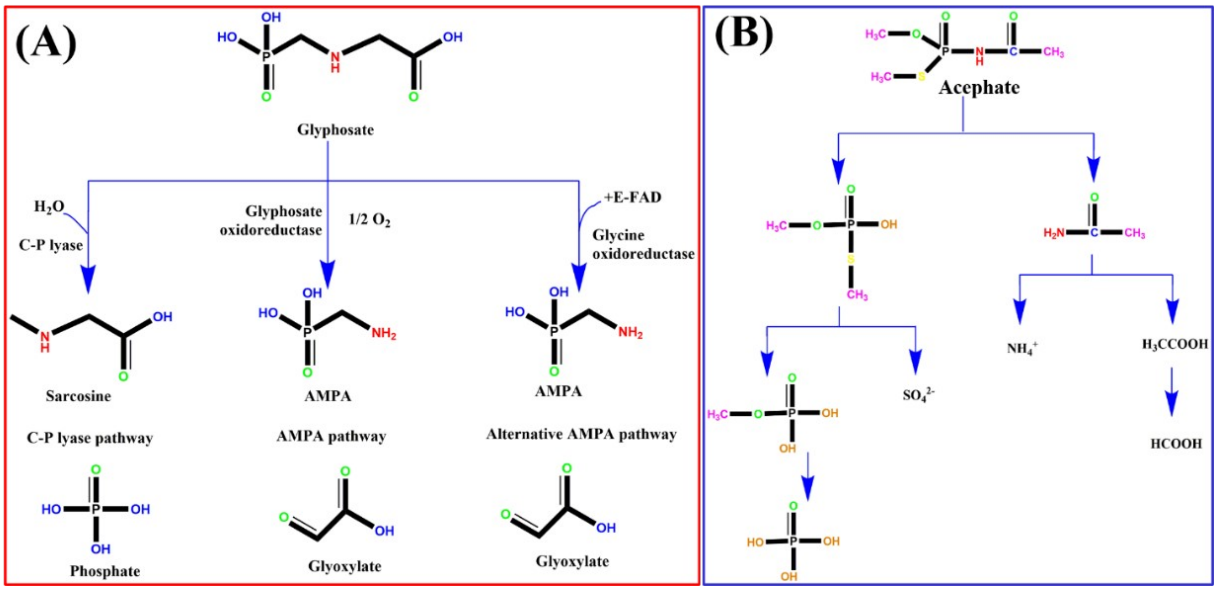

Figure. S15. Proposed Degradation pathways for GLY (A) and ACPH (B) degradation.

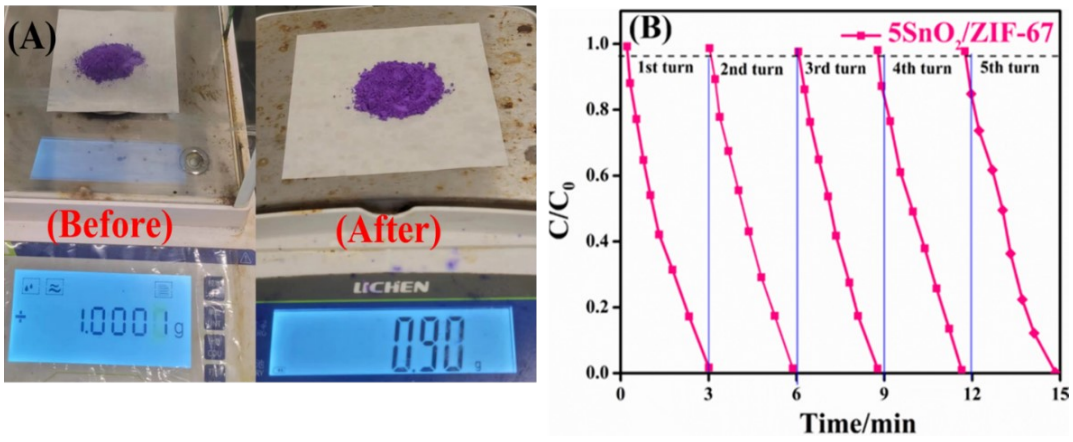

Figure. S16. Degradation activity stability (A), and recyclability test (B) of $5SnO_2$/ZIF-67 nanocomposite.

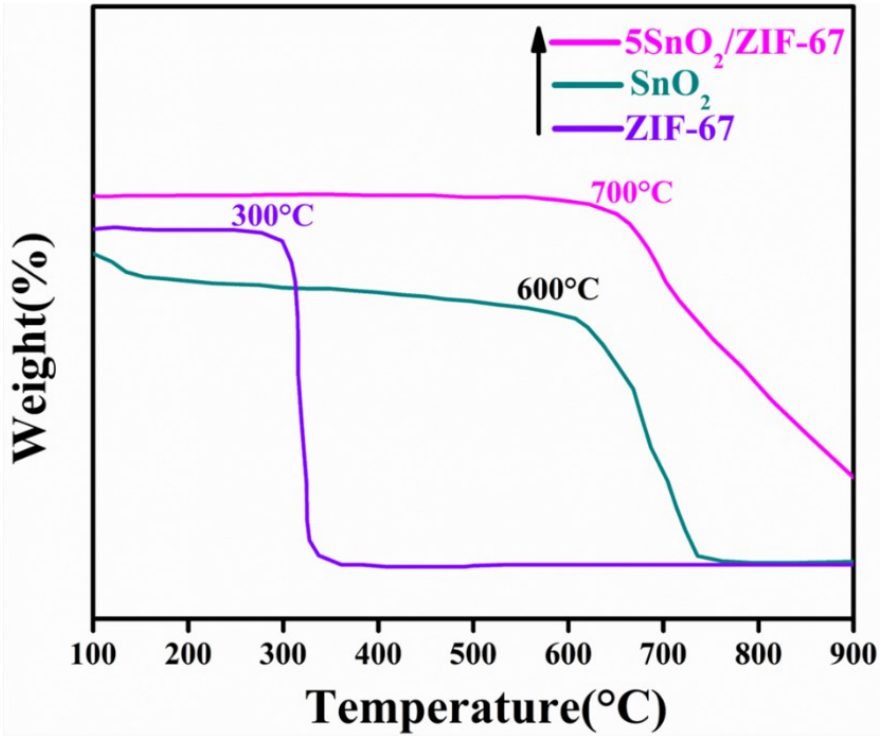

Figure. S17. TGA for ZIF-67, SnO_2, and $5SnO_2$/ZIF-67 nanocomposite.

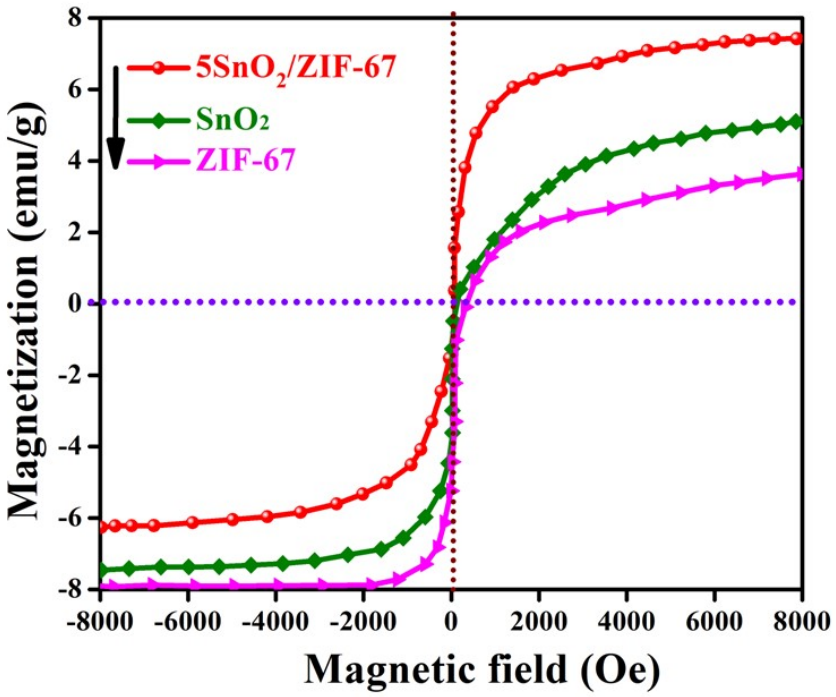

Figure. S18. Electron Paramagnetic Resonance Spectroscopy (EPR) of ZIF-67, SnO_2, and $5SnO_2$/ZIF-67 nanocomposite.

3. Supporting Tables (S1)

Table S1. Chemicals and Reagents Purity, Chemical/Mass formula, CAS Number, and Supplier Company Information

Component	Chemical Formula	CAS Reg. No	Suppliers	Mass Purity
Deionized water	DIH_2O	7732-18-5	Aladdin Industrial Corporation Shanghai	99.9
Methanol	C_3H_7OH	67-56-1	Tian in Fuyu fine chemical Co., Ltd	99.9
Zinc nitrate hexahydrate	$(Zn(NO_3)_2 .6H_2O$	10196-18-6	Aladdin Industrial Corporation Shanghai	≥99.5
Cobalt (II) nitrate hexahydrate	$(Co(NO_3)_2$	10026-22-9	Aladdin Industrial Corporation Shanghai	99.0
2-methylimidazole	$C_4H_6N_2$	CID 12749	Aladdin Industrial Corporation Shanghai	99.0
Nickel acetate tetrahydrate	$Ni(AcO)_2 \cdot 4H_2O$	6018-89-9	Aladdin Industrial Corporation Shanghai	99.0
Dihydroxybiphenyl-2,2'-dicarboxylate	$C_{14}H_8O_6$	97 92-88-6	Aladdin Industrial Corporation Shanghai	99.0
N, N-dimethylformamide	$(CH_3)2NC(O)H$	68-12-2	Aladdin Industrial Corporation Shanghai	99.9

Zirconium tetrachloride	$ZrCl_4$	10026-11-6	Aladdin Industrial Corporation Shanghai	99.9
Hydroxy terephthalic acid	$C_8H_6O_5$	636-94-2	Aladdin Industrial Corporation Shanghai	99.9
Tin (IV) chloride pentahydrate	$SnCl_4$	10026-06-9	Aladdin Industrial Corporation Shanghai	99.9
Ethanol	C_2H_5OH	64-17-5	Aladdin Industrial Corporation Shanghai	95.6
E. coli	DH5α	AB 204033	Biotechnology Department of Northeast Agricultural University, China	99.0
A. niger	CBS 513.88	ATCC90029	Biotechnology Department of Northeast Agricultural University, China	99.0
S. aureus	MRSA252	ATCC25923	Biotechnology Department of Northeast Agricultural University, China	99.0
Glyphosate	$C_3H_8NO_5P$	1071-83-6	Aladdin Industrial Corporation Shanghai	99.8
Acephate	$C_4H_{10}NO_3PS$	30560-19-1	Aladdin Industrial Corporation Shanghai	99.8